The distinction between object recognition and object identification in brain connectivity for brain-computer interfaces applications

Daniel Leong, Thomas Do and *Chin-Teng Lin, *Fellow, IEEE*

***Abstract*—Object recognition and object identification are complex cognitive processes where information is integrated and processed by an extensive network of brain areas. However, although object recognition and object identification are similar, they are considered separate functions in the brain. Interestingly, the difference between object recognition and object identification has still not been characterized in a way that brain-computer interface (BCI) applications can detect or use. Hence, in this study, we investigated neural features during object recognition and identification tasks through functional brain connectivity. Our aim is to discover a reliable feature that might be used to distinguish between object recognition and identification. The results demonstrate a significant difference between object recognition and identification in the participation coefficient and clustering coefficient of delta activity in the visual and temporal regions of the brain. Further analysis at the category level shows that this coefficient differs for different categories of objects. Overall, what we have found is a feature that might be able to be used to differentiate between object recognition and identification within a BCI object recognition system. Further, it may help BCI object recognition systems to determine a user's intentions when selecting an object.**

***Index Terms*—brain-computer interfaces (BCIs); object identification; object recognition; electroencephalogram (EEG); functional connectivity**

I. Introduction

Humans must process a vast amount of dynamic visual information in daily life. Simply to interact with the environment, visual information about our surroundings must be recognized and quickly processed by our visual system. Phenomenally, the human brain can search and detect a target in a panorama of complex natural images with astounding speed and excellent accuracy. Although many studies have attempted to solve the mystery of how the brain's visual system works, researchers still do not fully understand this complex system [1]. However, an increasing number of researchers are seeking to use our ever-advancing technology to study and improve our current understanding of the brain's visual system .

Currently, there are numerous hypotheses and theories regarding object recognition in the human brain, including viewpoint-invariant theory [2], viewpoint-dependent theory [3] and multiple views theory [4]. However, due to the complexity of the brain, none of these theories have yet been proven to explain how object recognition works in the human brain. However, one hypothesis has been widely accepted as the prominent model of how the brain neurally processes vision; it is known as the two-streams hypothesis [5]. The two-stream hypothesis holds that the visual processing of objects can be divided into two pathway streams: the dorsal stream and the ventral stream. The dorsal stream receives visual information in the occipital lobe, which then travels to the parietal lobe. This is visual-spatial information that measures an object's location relevant to the viewer. By contrast, the ventral stream receives visual information in the occipital lobe, after which it travels to the temporal lobe and is used for object recognition and identification. This phenomenon of the ventral stream has been illustrated using fMRI and MEG ([6], [7]), emphasizing the relationship between the ventral stream and object recognition in the human brain. This research is inspired by the two-streams hypothesis, focusing on analyzing the brain regions that are involved in the hypothesis.

Researchers have decoded a great amount of brain signals in their attempts to find a feature that can be used to represent the status of object recognition and identification. Among these attempts, functional connectivity has become a favoured measurement for object recognition due to its ability to reflect distinct connectivity patterns within the brain, also known as brain network properties [8]. By examining brain network properties, it is thought that we can better understand the underlying mechanisms of how the brain processes visual information [9]. There is evidence for the relationship between object recognition and network integration [10], which is an essential attribute of brain network properties. For instance, it has been shown that patients with psychosis and visual hallucinations have impaired functional connectivity in the visual network, possibly with a specific focus on the ventral attention network [11]. Also, research has demonstrated that early visual deprivation can lead to decreased functional

This work was supported in part by the Australian Research Council (ARC) under discovery grants DP180100656 and DP210101093. Research was also sponsored in part by the Australia Defense Innovation Hub under Contract No. P18-650825, US Office of Naval Research Global under Cooperative Agreement Number ONRG - NICOP - N62909-19-1-2058, and AFOSR – DST Australian Autonomy Initiative agreement ID10134. We also thank the NSW Defense Innovation Network and NSW State Government of Australia for financial support in part of this research through grants DINPP2019 S1-03/09 and PP21-22.03.02.

D. L., T. D. and C.-T. L. are with University of Technology Sydney, Faculty of Engineering and Information Technology, Australian Artificial Intelligence Institute and Human-centric Artificial Intelligence Centre, 15 Broadway, Ultimo, New South Wales 2007, Australia.

*Corresponding authors: Chin-Teng Lin (e-mail: Chin-Teng.Lin@uts.edu.au)

connectivity between the occipital visual cortices and the parietal somatosensory, frontal motor, and temporal multisensory cortices [12].

Nevertheless, the majority of studies on functional connectivity have been conducted using functional magnetic resonance imaging (fMRI) due to its high spatial resolution. This has allowed researchers to observe changes in the brain's regions in a great deal of definition. However, electroencephalogram (EEG) provides a better temporal resolution. With EEG, information can be gathered over much smaller time intervals, which is not achievable with an fMRI [13]. In fact, EEGs are the ideal measurement tool for collecting information related to specific events, such as object recognition. Recently, EEG signals have been used for functional connectivity studies in order to investigate specific brain regions related to object recognition. For example, a study by Rizkallah et al. [14] investigated changes in the dynamic brain network modularity while participants recognized meaningful and meaningless visual images using EEG-based functional connectivity. Another two studies ([15], [16]) provided a result that showed the change in functional connectivity during object-related tasks in patients with Alzheimer's disease using EEG. In addition to detecting changes in the brain network, EEG-based functional connectivity has also been used to classify different object categories in BCI research. An example comes from a study by Tafreshi, Daliri & Ghodousi [17], where they attempted to use EEG features extracted with functional and effective connectivity techniques and then use these features to classify 12 different categories of the object.

Most of the EEG-based object recognition studies have similar experimental designs where the participant must press a button when a target stimulus appears. The target stimuli are the focus of these studies. Often they are keywords that relate to the target object, such as its category [17] or the test gauges the meaningfulness [14] or ambiguity [18] of the object. There are a few studies, however, that have altered the experimental design to try and detect object identification in the brain as opposed to object recognition. Although object recognition and object identification are comparable, object identification is considered to be an individual process where different regions of the brain are involved in processing the information [19]. For instance, a study by Dyck & Brodeur [18] included an object identification experiment where the participants were asked to observe several images of a target object in different scenarios. The task required the participants to identify all the objects in the scene and detect the target object within it. Another example comes from a study by Ra¨ma¨ & Baccino [20], where the participants were asked to identify chimerical objects. Chimerical images are constructed by joining two halves of an original drawing while keeping the lines unbroken and continuous. What these studies have shown is that the difference between object recognition and identification largely depends of the number of objects presented to a person. When presented with just one object, people will use object recognition, but when asked to distinguish between many objects, a person will draw on object identification.

Several researchers have attempted to create a BCI object identification system with prominent EEG features. For instance, the current P3-based BCI detects object identification based on the P3 peak, which happens around 300-500 ms after event onset ([21], [22]). However, this P3-based BCI paradigm relies on the onset of the visual stimulus to elicit the P3 response, such as a flash or flashes over the object of choice. Besides the P3 peak, steady state visually evoked potential (SSVEP) is also a widely used feature for BCI-based object identification. This system puts a flicker at a specific frequency over the object of choice [23], [24], [25]. In terms of BCI-based object recognition systems, researchers commonly use EEG features to classify a target object based on a category. A commonly used EEG feature is event-related potential (ERP), which is the brain's response to a specific event that has occurred. ERPs are measured when an object appears in the participant's field of view and then is classified based on the category of the object [26], [27], [28]. In addition to ERP, EEG features such as event-related spectral perturbation (ERSP) [29] and functional and effective connectivity features [17] have also been tested for BCI-based object recognition. Despite advancements in the development of BCI systems capable of differentiating between object recognition and object identification, these technologies predominantly remain in nascent stages, not yet suitable for practical application. The primary challenge lies in the system's inability to ascertain the user's intent in targeting an object: is the objective to enable the BCI to recognize the object (object recognition), or is it to prompt the BCI to select an object within the user's surroundings (object identification)? Once the intention of the user is detected, the BCI system can initiate the algorithm specifically designed for either object recognition or object identification.

Therefore, with this study, we looked for a neural feature or features that might help us distinguish between the two processes of object recognition and object identification. Our aim was to identify a reliable feature that might be applied in a BCI application to help the system understand the user's objective when selecting a target object.

II. Methodology

A. Participant and Data Recording

The experiment involved 25 participants (aged 32.5± 10.4 years), with each participant completing a total of 600 trials. All participants reported normal or corrected-to-normal vision. The experiment took place at the Computation Intelligence and Brain-Computer Interface (CIBCI) Centre located in University of Technology Sydney (UTS). Every participant was first provided with instructions about the experiment and then asked to sign a consent form before participating. Ethics approval was issued by the University of Technology Sydney under ethics ID ETH20-5519. Brain activity was recorded using a 64-channel EEG system from Neuroscan, Compumedics,

Australia. This is a medical-grade device that provides high-density EEG recordings with great accuracy. It has been used in numerous studies in neuroscience and neurodiagnostics. The EEG electrode placement was consistent with the extended 10-20 international system. Data were referenced to an electrode located closest to the standard position FCZ. The contact impedance of the electrode was maintained below 5k, and the EEG recordings were digitally sampled at 1000 Hz.

B. Experimental Design

The participants in our experiment were asked to perform an object recognition task and an object identification task. In the object recognition task, they were shown an image selected at random from the Caltech-256 object category dataset [30]. Images from four different categories were included in the trial: animals, flowers, food, and vehicles. Each category contained five different types of objects, and each type of object contained ten images. Thus, a total of 200 images were used in the experiment. (see Fig.1). Each trial started with the participant looking at a picture of their target object for 1 second. They were then asked if the image belonged to its category. For example, if the target image was of a bear, the participant was asked: "animal?" and they had 2 seconds to answer. This question was asked so the researchers could determine whether or not the subject had accurately recognized the target image.

Next, we administered the object identification task. Four images were randomly chosen from the image dataset but at least one image was chosen from the same category and subtype as the target image from the previous recognition task. The four images were placed in four different directions (up, down, left and right), and the participants had to press the button corresponding to the image that was most closely related to the target image. Note that, because the images were chosen at random, it was possible for there to be choices of the same category and subtype (see the bottom row of Fig. 1). However, the subjects only had to choose the one they felt most closely matched their target image. The participants had 3 seconds to respond. Thus, each trial lasted six seconds: the target image would appear for one second, followed by the question with two seconds to respond. Then, the four images appeared with three seconds to respond. Before the target image appeared, a fixation cross was displayed for 300 ms. This served as the trial's baseline. Fig. 1 shows an example trial.

C. EEG Analysis

The recorded EEG signals were processed using EEGLAB v14.1.2 [31], a toolbox in MATLAB. The raw EEG data were filtered using a 1Hz high-pass and a 50Hz low-pass finite impulse response (FIR) filter and then down-sampled to 250 Hz. After removing the noisy channels, the data were re-referenced to the average. Then, adaptive mixed independent component analysis (AMICA) was applied to the re-referenced data to decompose them into maximally independent components (ICs), which are statistically independent sources of the variance in the EEG. Any independent components (ICs) related to eye movement, muscle activity and other noise were rejected using the IClabel toolbox [32]. Once these bad components had been rejected, we extracted the epochs. An epoch began 300 ms prior to the target image appearing (i.e., event onset) and ended 5 seconds after the target image appeared. Thus, the whole duration of the trial was covered. Bad epochs were then identified by checking their data values. It would be removed if the epoch contained data values outside a given standard deviation threshold (threshold =150 uV).

The extracted epochs were divided into two parts: the object recognition portion of the trial (from when the target image first appeared) and the object identification portion of the trial (from when the four images appeared). The epoch data from each participant were then grouped together based on the four image categories. Thus, we analyzed eight conditions: object recognition (ATOR, FOTOR, FTOR and VTOR) and object identification (ATOI, FOTOI, FTOI and VTOI) in each of the four categories of objects.

D. Functional Connectivity and Network Properties

To tackle the inverse problem of EEG, distributed source localization was used. Further, functional connectivity was estimated using the Brainstorm toolbox [33]. The distributed brain source localization activity was estimated from the data epochs, and then the brain functional connectivity was estimated from the source activity. Initially, the data epochs were co-registered with the MRI template [34] and the EEG sensor locations in the same anatomical landmarks. The openMEEG [35] process was then used to estimate the lead field of the cortical mesh. Meanwhile, a noise covariance matrix was calculated using the fixation cross period of the trial. EEG data were then projected onto an anatomical framework consisting of 68 cortical regions as identified by means of re-segmenting the Desikan-Killiany Cortical Atlas [36] using FreeSurfer [37]. Next, the standardized low-resolution brain electromagnetic tomography (sLORETA) method [38] was used to reconstruct the regional time series from the 68 brain regions. Amplitude envelope correlation (eq. 1) [39] (AEC) was then used to estimate the functional connectivity between cortical regions, resulting in a 68 $\times$ 68 connectivity matrix. Furthermore, we restricted the analysis to the delta (1–4 Hz), theta (4–8 Hz), alpha (8–12 Hz), beta (12–30 Hz), low gamma (30-60 Hz) and high gamma (60-90 Hz). In alignment with the findings from pertinent research on functional connectivity [40], [9], [41], [42], [43], the aforementioned connectivity matrix underwent proportional thresholding. We implemented a threshold of 10% of the highest AEC values to preserve only the most significant functional connections. Subsequently, the remaining AEC connectivity matrices that did not meet this criterion were excluded from the analysis.

$$\tilde{x}(t) = x(t) + j\mathcal{H}\left\{x(t)\right\} = a_{\tilde{x}}(t)e^{j\phi_{\tilde{x}}(t)} \tag{1}$$

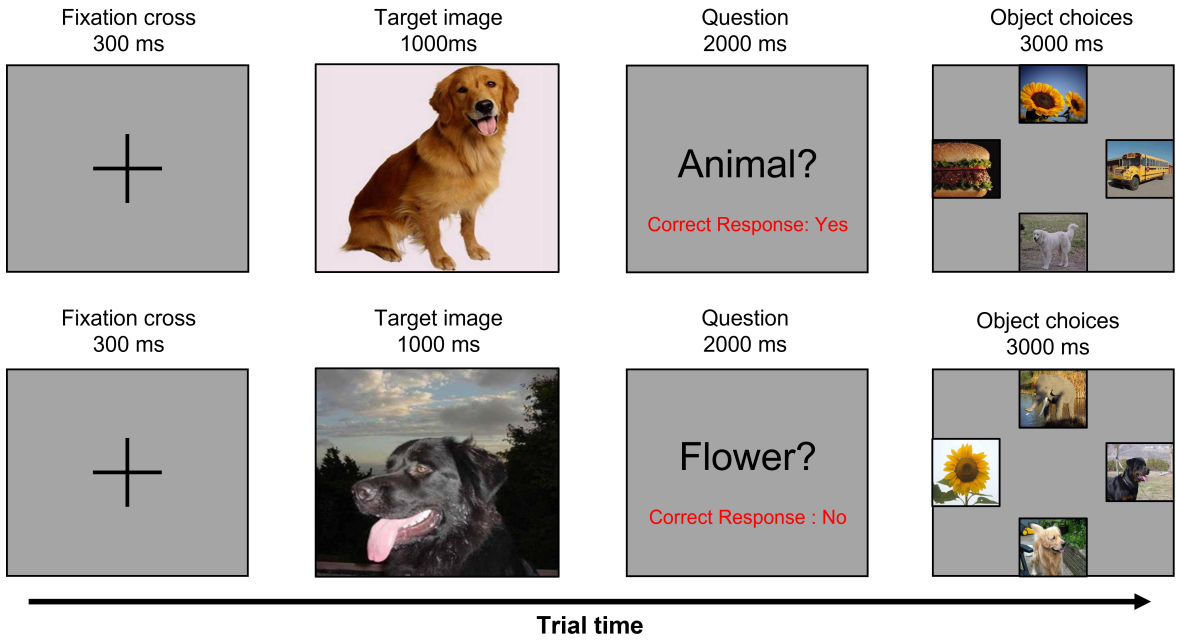

Fig. 1: The experimental design. All trials began with a fixation cross lasting for 300 ms, followed by the target image appearing for one second. After the appearance of the target image, the participants were asked what the object was of and given two seconds to respond. Subsequently, four images were displayed with at least one image chosen from the same category and subtype as the target image. The participants had three seconds to select the object that most closely resembled their target object by pressing a button in the corresponding direction (up, down, left and right). The top half of the figure shows an example of the trial with the correct response to the question (text in red) and the layout of the object choices. The bottom half shows an example of the trial with two possible options for the most closely matching object.

$\tilde{x}(t)$ is a complex time series uniquely associated with the original data time series, $x(t)$. The real part of $\tilde{x}(t)$ is the original time series $x(t)$, and the imaginary part is the Hilbert transform of that same time series $\mathcal{H}\{x(t)\}$. Module $a_{\tilde{x}}(t)$, and Phase $\phi_{\tilde{x}}(t)$ correspond to the instantaneous amplitude (or envelope) and instantaneous phase of the original time series $x(t)$, respectively.

Utilizing the selected AEC connectivity matrix, the network properties of the brain were calculated at each frequency of each condition. In terms of the experimental task, network integration was chosen as our measurement because it indicates the global information exchanged at each node (each cortical region). The network properties were calculated for all eight conditions of each participant, and then a statistical test was conducted to compare the difference between them. We used the Brain Connectivity Toolbox [44] to calculate the network properties along with the participation coefficient (Eq. 2) and clustering coefficient (Eq. 3). This participation coefficient is a measurement that reflects global information processed in each region of the brain [45], and it will be used to estimate the integration. The clustering coefficient, which reflects local information processing in each region, will be utilized to estimate segregation[46]. The full pipeline of the analysis is described in Fig. 2.

$$P_i = 1 - \sum_{s=1}^{N_m} \left(\frac{k_{is}}{k_i}\right)^2 \tag{2}$$

k_{is} is the number of edges between node i, Nm is the number of module and the other nodes in module s, and k_i is the total degree of node i. The participation coefficient of a node is close to 0 if all of its links are within one module and close to 1 if its links are evenly distributed among all the modules.

$$C_i = \frac{2t_i}{k_i(k_i-1)'} \tag{3}$$

The clustering coefficient is calculated as the proportion of links among a node's neighbours divided by the number of connections that could potentially exist between them. The number of triangles around node i is represented by t_i, and the number of edges connected to node i is indicated by k_i. The clustering coefficient is 0 if there are no connections and 1 if all neighbours are connected.

E. Binary classification

Subsequent to the computation of brain connectivity features for all participants, a binary classification analysis (distinguishing between object recognition and object identification) was performed using a variety of classifier models and ensemble learning techniques. This binary classification was performed individually for each category of objects, with the intention of assessing the efficacy of brain connectivity features across different object types. Upon meticulous evaluation, the most effective models were identified as Adaptive

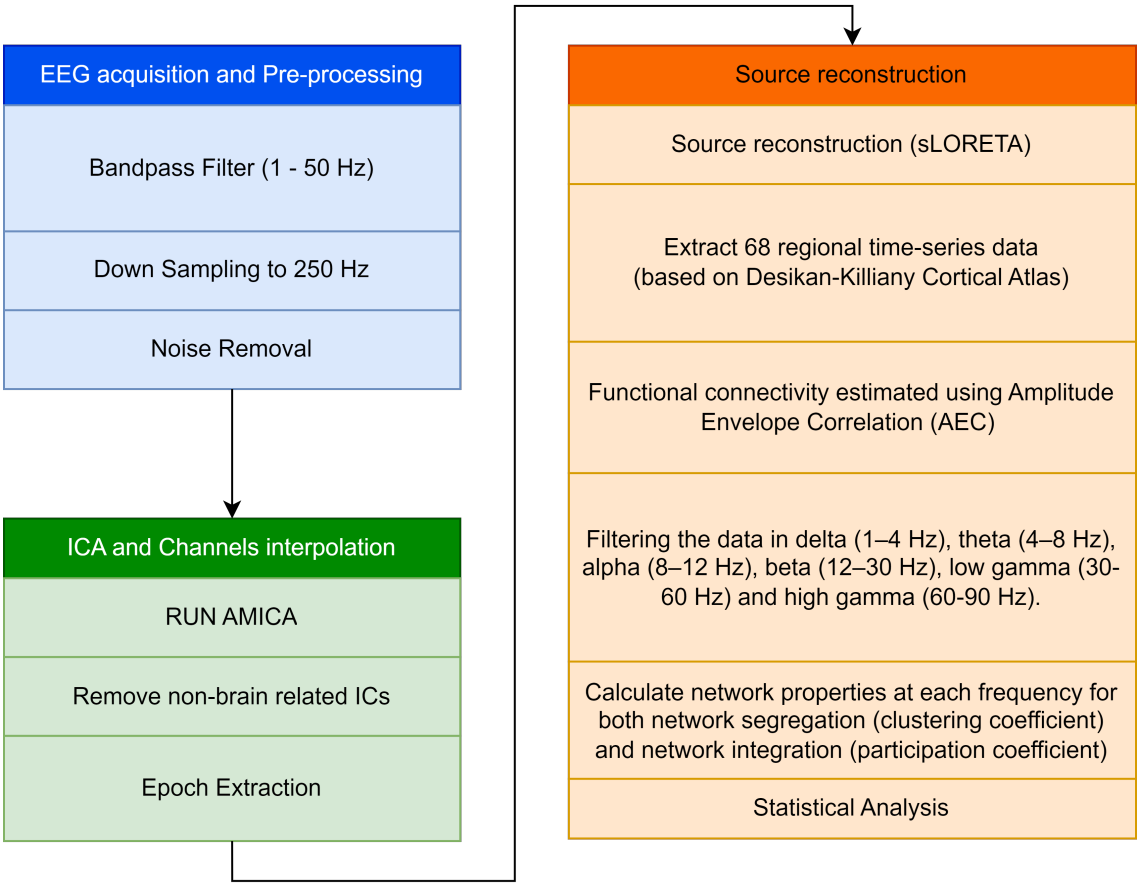

Fig. 2: Data processing pipeline for Functional connectivity analysis.

Boosting (AdaBoost), K-Nearest Neighbors (KNN), Random Forest (RF), Multi-Layer Perceptron (MLP), Support Vector Machine (SVM), and XGBoost with Tree Booster (XGBTree). These models were sourced from the scikit-learn library [47] for implementation in the Python programming language. The hyperparameters for each model were fine-tuned using Bayesian optimization [48]. Specific optimizations included the number of estimators and learning rate for AdaBoost; the number of neighbours for KNN; the number of trees and maximum tree depth for RF; the size of the hidden layer and initial learning rate for MLP; the regularization parameter and kernel coefficient for SVM; and the number of trees, maximum tree depth, learning rate, gamma, the minimum child weight, subsample ratio of the training instances and columns when constructing each tree for XGBTree. Additionally, to assess the performance of these models, a ten-fold cross-validation approach was employed.

III. Results

The data for all 25 participants were used to get every participant's functional connectivity result, with the data divided into four groups, one for each category, and then subdivided into the eight classes mentioned in the methodology. We calculated the participation coefficients and clustering coefficients. Significant differences in participation and clustering coefficients across these tasks and classes were first assessed via the Friedman test, followed by a post-hoc pairwise Wilcoxon signed-rank test. Out of all the tested frequency bands, the results revealed significant differences in the delta activity of the brain's visual and temporal regions. Fig.3A&B shows the results of the Wilcoxon tests for the participation coefficients of the two tasks as observed in the visual region (OI and OR, $p = 0.00881$) and in the temporal region (OI and OR, $p = 0.0137$). Furthermore, Fig.3C&D shows the results of the Wilcoxon tests for the clustering coefficient in both visual (OI and OR, $p = 0.0161$) and temporal region (OI and OR, $p = 0.126$).

Fig. 4A shows the results of the Wilcoxon tests for the eight classes in the visual region. Significant differences in the participation coefficients for delta activity were found between the recognition and identification tasks for the following categories: animals (ATOI and ATOR, $p = 0.019$), food (FOTOI and FOTOR, $p = 0.005$) and flowers (FTOI and FTOR, $p = 0.039$). Fig. 4B shows the results for the temporal region. Here, there were significant differences in the animal (ATOI and ATOR, $p = 0.034$), flower (FTOI and FTOR, $p = 0.019$) and vehicle (VTOI and VTOR, $p = 0.045$) categories. For the clustering coefficient, Fig. 4C shows the results of the Wilcoxon tests in the visual region. Significant differences were observed in the categories of flower (FTOI and FTOR, $p = 0.019$) and vehicle (VTOI and VTOR, $p = 0.045$). Fig.

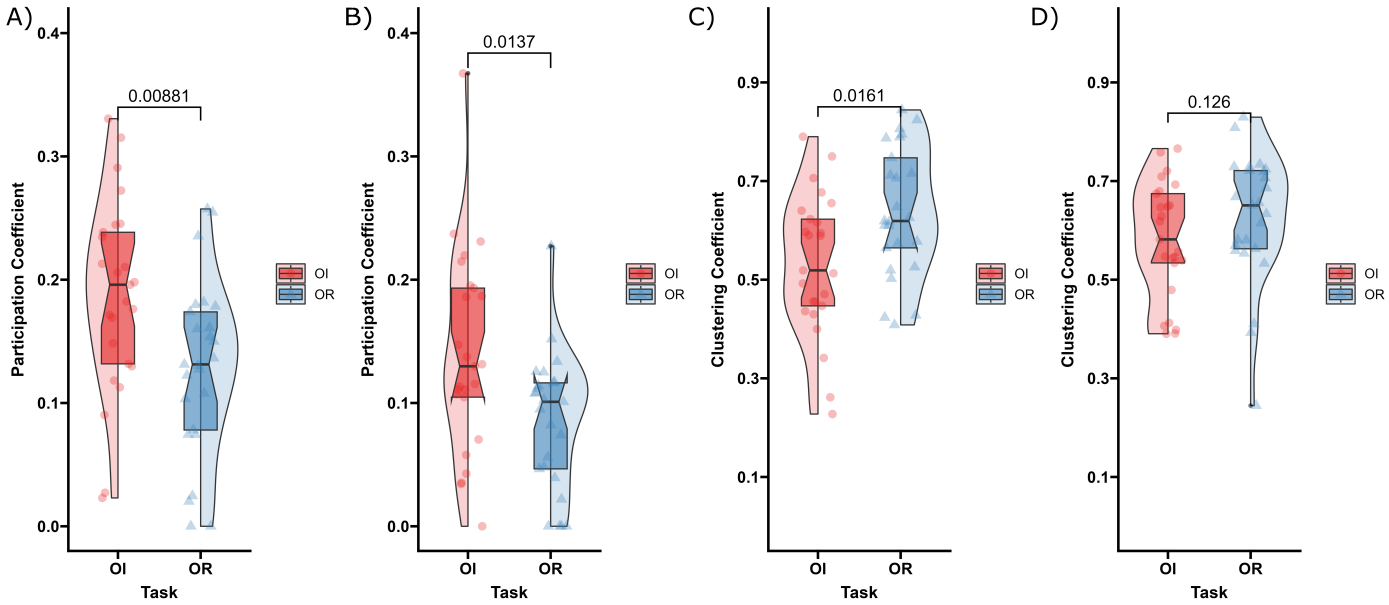

Fig. 3: Graph properties at visual (A&C) and temporal (B&D) regions: participation coefficient and clustering coefficient between object recognition and identification task in delta frequency. Pairwise post-hoc Wilcoxon signed-rank tests were used to check for significant differences between tasks.

4D shows the results for the temporal region, and significant differences were observed in the animal (ATOI and ATOR, p = 0.019) and flower (FTOI and FTOR, p = 0.045) categories.

The result of the binary classification of object recognition and identification is shown in Table I. This classification was performed for each category using three distinct combinations of brain connectivity features: Participation Coefficient only (PC), Clustering Coefficient only (CC), and a combination of both (PC&CC). In the classification of various categories, the animal category exhibited the highest accuracy and F1 score, achieving 80% and 0.78, respectively, when employing both the participation coefficient and clustering coefficient with the KNN classifier. The food category, when classified using the AdaBoost and KNN classifiers, achieved an accuracy of 60% and an F1 score of 0.71. For the flower category, the most effective classification result was achieved using both the Participation Coefficient and Clustering Coefficient in conjunction with the RF classifier, yielding an accuracy of 72.5% and an F1 score of 0.70. Lastly, the vehicle category recorded an accuracy and F1 score of 75% and 0.8, respectively, when the classification was conducted using the Participation Coefficient in combination with the XGBTree classifier.

We further visualized the functional connectivity results using BrainNet Viewer [49], plotting a full view of the graph properties (lateral, medial, ventral and dorsal) for the object identification task in Fig. 5 and the object recognition task in Fig. 6. An axial view of the graph properties for the eight classes follows in Fig. 7. The node, the blue dot in the functional connectivity map, indicates the brain regions or regions of interest that are defined based on anatomical or functional criteria. The node size represents the degree of activity or connectivity of a particular region, with larger nodes representing more active regions. On the other hand, The red lines connecting each node represent the edge, which states the strength of the connection between the two nodes.

IV. Discussion

Object recognition and object identification are essential aspects of many daily activities. Both require us to process a vast amount of dynamic visual information and recall information from memory quickly and precisely. This study explores these processes in a combined task of object recognition and object identification by observing differences in the functional connectivity of the brain. We found that the differences in functional connectivity between the object recognition task and the object identification task occur at visual and temporal integration. Visual and temporal integration is higher during object identification in the delta band as measured by the AEC connectivity matrix. This finding could be an indicator for distinguishing between object recognition and object identification in BCI systems.

A. Significance of low-frequency signal

The low-frequency signal in the human brain has revealed its function/reflection in object recognition [50]. Moreover, this characteristic has been reported in both healthy people and in patients. For instance, Behroozi et al. [29] conducted an object recognition experiment with ten healthy participants and found that the phase patterns of EEG signals across time in the delta band could be used to discriminate between different objects. In patients with attention deficit hyperactivity

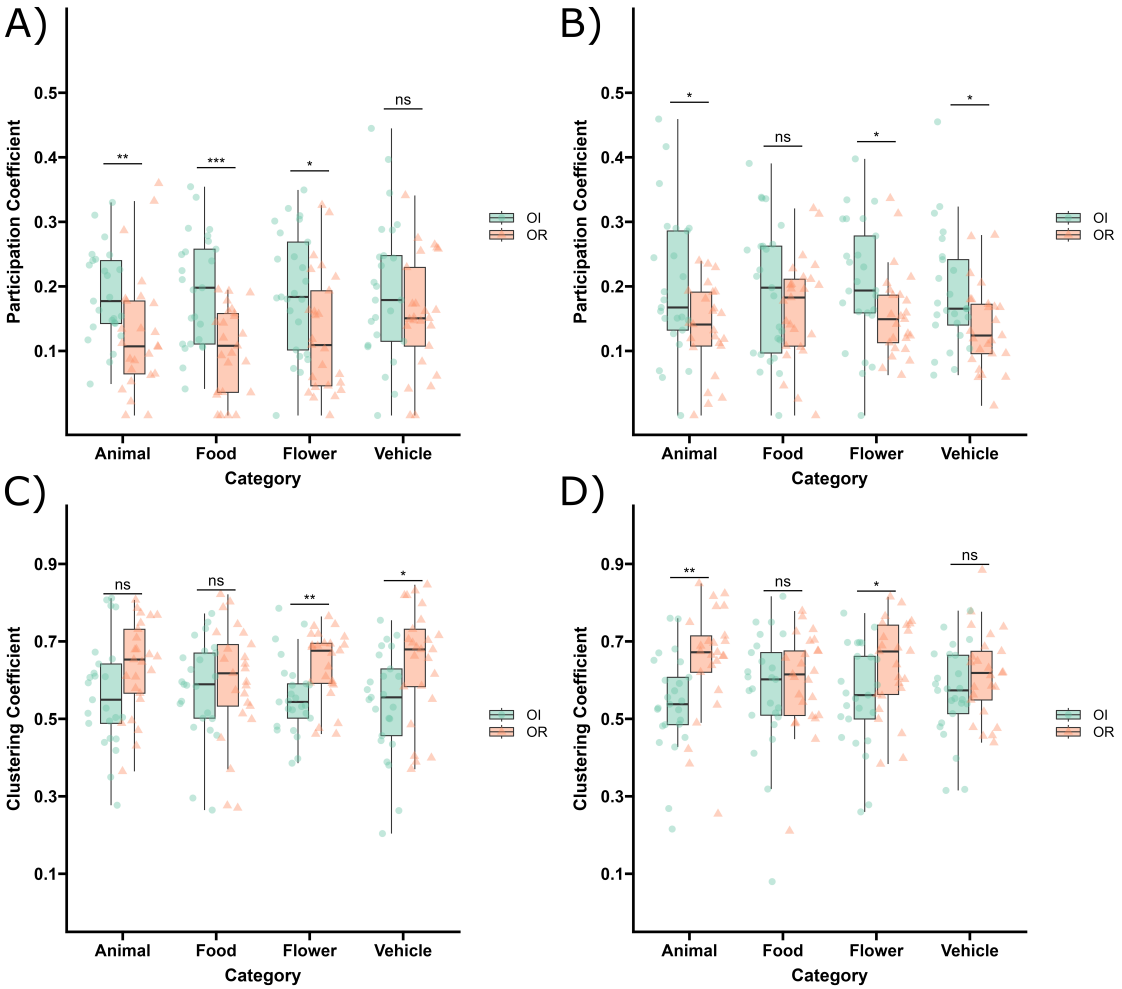

Fig. 4: Graph properties in the visual (A&C) and temporal (B&D) regions of the brain. The participation coefficients and clustering coefficient for four categories during object recognition and identification tasks in the delta frequency. Pairwise post-hoc Wilcoxon signed-rank tests were used to check for significant differences between classes (* and ** indicate $p<0.05$ and $p<0.01$, respectively).

disorder (ADHD) [51], the delta EEG bands highlighted essential features for classification between both the ADHD group and the control group. This is further evidence of how the low-frequency EEG power bands might serve as potential markers of a visual processing deficit in people with ADHD. Furthermore, Watrous et al. [52] conducted an experiment involving an object recognition task with six patients with medication-resistant epilepsy. They found that phase-amplitude coupling (PAC) supports phase-dependent stimulus representations for object categories, and that PAC was most prevalent in the delta band. Some studies have reported the usefulness of the delta band frequency as a feature for identifying the object recognition phenomenon in studies of EEG-based object recognition and object identification. For example, Cao et al. [53] attempted to create a computer-aided design (CAD) program for determining a person's intention to select an object based on EEG signals in four frequency bands. They found that the weights trained from the data of the delta band were significantly higher than those from the high-frequency band (beta), thus increasing the classification accuracy of object selection. Nevertheless, there is limited information on the delta features of brain connectivity in EEG studies.

B. Functional Connectivity

Research has been undertaken on brain connectivity using EEG data, but the findings of these studies cover the whole brain network, not the specific regions of the brain relating to object recognition tasks. Therefore, we undertook to investigate brain participation in the visual and temporal cortices. It is well-understood that object perception occurs predominantly in the visual cortex [54], while object identification primarily takes place in the temporal cortex [55], with both processes occurring in the low-frequency band. However, our results from this study demonstrate that low-frequency signals in the visual and temporal cortices might be used as a feature to distinguish between object recognition and identification processes in the human brain (Figs. 3 and 4).

TABLE I: Binary classification results for each category with different combinations of brain connectivity features

Animal PC

Classifier	Accuracy	F1-Score
AdaBoost	50%	0.54
KNN	75%	0.78
MLP	60%	0.67
RF	65%	0.70
SVM	60%	0.67
XGBTree	65%	0.69

Animal CC

Classifier	Accuracy	F1-Score
AdaBoost	50%	0.51
KNN	60%	0.63
MLP	65%	0.70
RF	55%	0.57
SVM	65%	0.67
XGBTree	65%	0.70

Animal PC&CC

Classifier	Accuracy	F1-Score
AdaBoost	70%	0.625
KNN	80%	0.78
MLP	70%	0.67
RF	75%	0.71
SVM	72.5%	0.68
XGBTree	72.5%	0.69

Food PC

Classifier	Accuracy	F1-Score
AdaBoost	60%	0.71
KNN	60%	0.71
MLP	60%	0.67
RF	55%	0.67
SVM	60%	0.67
XGBTree	60%	0.71

Food CC

Classifier	Accuracy	F1-Score
AdaBoost	35%	0.38
KNN	35%	0.35
MLP	40%	0.45
RF	30%	0.41
SVM	40%	0.39
XGBTree	40%	0.45

Food PC&CC

Classifier	Accuracy	F1-Score
AdaBoost	52.5%	0.45
KNN	55%	0.53
MLP	40%	0.40
RF	50%	0.5
SVM	40%	0.25
XGBTree	52.5%	0.61

Flower PC

Classifier	Accuracy	F1-Score
AdaBoost	65%	0.69
KNN	55%	0.64
MLP	55%	0.64
RF	55%	0.64
SVM	55%	0.64
XGBTree	65%	0.67

Flower CC

Classifier	Accuracy	F1-Score
AdaBoost	50%	0.58
KNN	50%	0.44
MLP	55%	0.47
RF	50%	0.58
SVM	55%	0.53
XGBTree	50%	0.58

Flower PC&CC

Classifier	Accuracy	F1-Score
AdaBoost	70%	0.67
KNN	62.5%	0.62
MLP	62.5%	0.57
RF	72.5%	0.70
SVM	62.5%	0.51
XGBTree	65%	0.71

Vehicle PC

Classifier	Accuracy	F1-Score
AdaBoost	55%	0.57
KNN	60%	0.56
MLP	70%	0.75
RF	55%	0.57
SVM	65%	0.78
XGBTree	75%	0.80

Vehicle CC

Classifier	Accuracy	F1-Score
AdaBoost	55%	0.61
KNN	50%	0.37
MLP	50%	0.5
RF	50%	0.60
SVM	55%	0.53
XGBTree	55%	0.52

Vehicle PC&CC

Classifier	Accuracy	F1-Score
AdaBoost	62.5%	0.67
KNN	65%	0.69
MLP	70%	0.71
RF	55%	0.47
SVM	70%	0.71
XGBTree	65%	0.68

Furthermore, we extend the investigation into the higher resolution of the task by looking into the differences between object recognition and identification in four categories. Previous studies have shown the significance of the visual and temporal regions for recognizing and discriminating between different shapes and objects ([56], [57], [6]). The results of this study have demonstrated significant differences in the participation coefficient and clustering coefficient of delta brain activity for object recognition versus object identification tasks in the visual region with the animal, food, and flower categories. This suggests that these categories are visually different enough for the participants to distinguish between objects at first glance. In the temporal region, we saw the same kinds of differences in the animal, flower, and vehicle categories, which implies that these image categories may require more complex processing of the brain.

The differences in the participation coefficient between the animal and flower categories across both brain regions are noteworthy. In terms of the clustering coefficient, differences were observed solely for the flower category across both regions. The difference in the animal category was restricted to the temporal region, with no corresponding variance observed in the visual region. Nonetheless, the animal category demonstrated a near-significant difference in the visual region ($p = 0.071$). This result suggests that these categories elicit a different type of response from participants, but, since we still do not fully comprehend the human brain, what these results indicate exactly is uncertain. However, there are some studies that might help us explain this phenomenon. For instance, these differences may be part of the brain's response to living objects. Farah and Rabinowitz [58] and Mahon et al. [59] both undertook research regarding the brain's response to living and non-living objects, and both found that living objects tend to be more evocative to humans than non-living objects.

For the food category, significant differences were only observed in the visual region regarding the participation coefficient. This phenomenon could be linked to the human instinct for food [60], which perhaps causes differences in the visual region to be more evident than in the temporal region. Lastly, in the vehicle category, we found significant differences in the temporal region regarding the participation coefficient and the visual region regarding the clustering coefficient. The ventral stream theory of visual processing may possibly explain this result. Since vehicles are complex objects, the brain may need to process large amounts of visual information in order to recognize the corresponding target in the object recognition task, hence the high clustering coefficient in the visual region. During the object identification task, when the participants saw the image of the vehicle

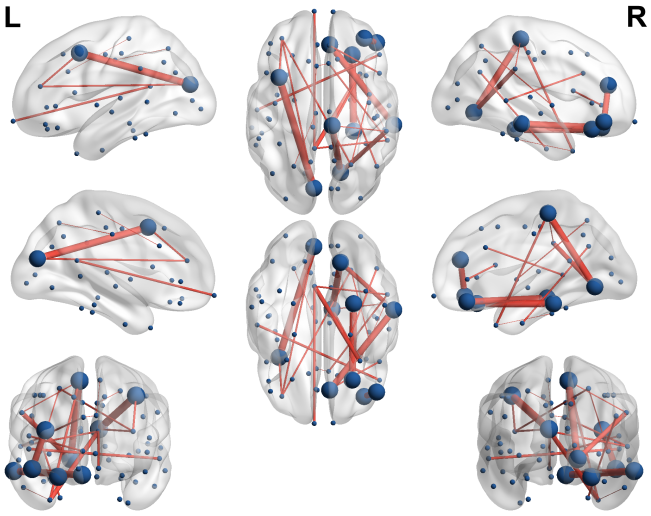

Fig. 5: Functional connectivity of the brain network during the object identification task. The nodes indicate brain regions (based on the 68 Desikan-Killiany Atlas). The edges indicate significant connections between nodes; the edge size indicates the strength of the connection.

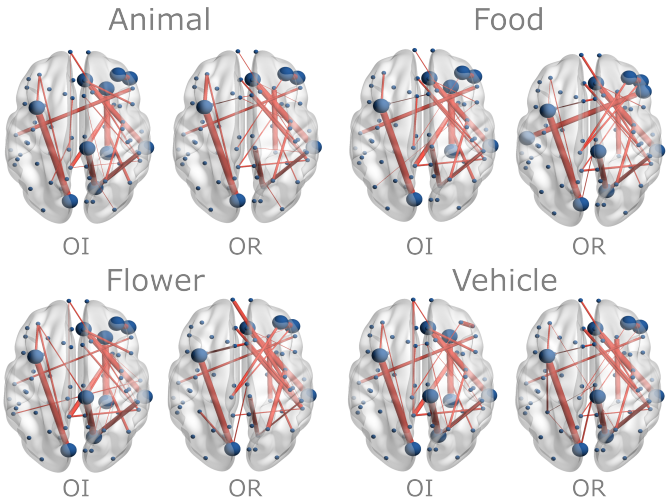

Fig. 7: Functional connectivity of the brain network across four categories during the object recognition and identification task. The nodes indicate brain regions (based on 68 Desikan-Killiany Atlas). The edges indicate a significant connection between nodes; the edge size indicates the strength of the connection.

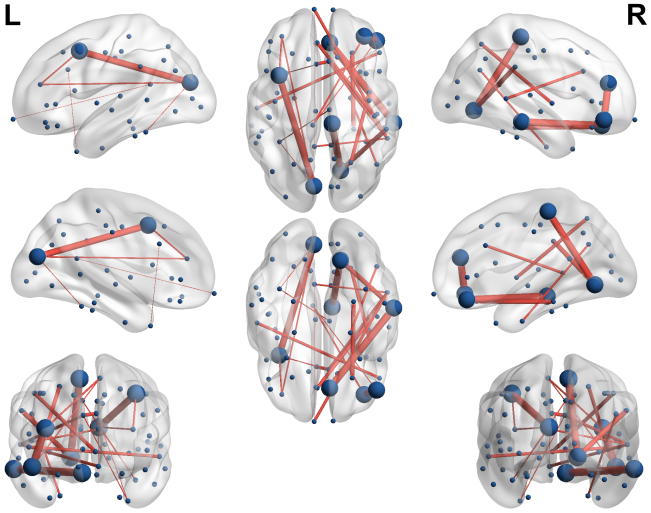

Fig. 6: Functional connectivity of the brain network during the object recognition task. The nodes indicate brain regions (based on the 68 Desikan- Killiany Atlas). The edges indicate a significant connection between nodes; the edge size indicates the strength of the connection.

presented to them within the choices, they noticed an object but did not know what it was until the visual information was transmitted to the temporal region and other brain regions that are associated with recognizing, recalling and locating the object. Therefore, the significant differences in participation coefficient between object recognition and object identification only occurred in the temporal region.

The participation coefficient measures the diversity of the intermodular interconnections of individual modules and provides insight into their functional role among their own module from multiple modules [44]. Conversely, the clustering coefficient measures the prevalence of clustered connectivity surrounding individual nodes [46]. Both the participation coefficient and clustering coefficient range between 0 and 1. If the participation coefficient is close to 0, the module only connects to a few modules and vice versa as it approaches 1. For the clustering coefficient, the connection between nodes within the module is weak as it approaches 0 and strong as it approaches 1. As demonstrated in Fig. 3, object identification has a higher participation coefficient than object recognition in every category. These high participation coefficients indicate that the functional integration in the brain is more robust during object identification tasks than object recognition tasks. Furthermore, it implies that there is less segregation between the modules in the visual and temporal regions during object identification tasks than during object recognition tasks. More generally, it means that the visual and temporal regions are more connected to each other and other brain regions during object identification. Ostensibly, object identification tasks require the participants to recognize, recall and identify similarities between selected images. Hence, the high participation coefficient in the visual and temporal regions may suggest that more brain regions beyond these two are also involved in object identification. Regarding object recognition, the clustering coefficient surpasses that of object identification in all categories. This high clustering coefficient signifies that functional segregation within the brain is more intense during object recognition tasks than object identification tasks. In object recognition tasks, the participants are solely required to recognize the object. The visual information is initially processed in the visual region to detect the object's features before transmitting these characteristics to the temporal region to determine the object's

identity. However, the same process is not precisely the same in the object identification task because object identification entails more than just recognizing the object, as previously mentioned. This phenomenon suggests that visual information is predominantly processed during object recognition tasks in the visual and temporal regions.

Furthermore, our comprehensive analysis, conducted at an enhanced resolution, is demonstrated through the functional connectivity map, as illustrated in Figures 5, 6, and 7. These figures reveal that nodes within the visual and temporal regions, quantified by the clustering coefficient, are notably larger, signifying the pivotal role of the visual and temporal regions in tasks related to object recognition and identification. Concurrently, the edges linked to the nodes in these regions, as measured by the participation coefficients, demonstrate robust connections, indicating significant interactions between the visual and temporal regions and other areas of the brain.

C. Binary classification

According to the binary classification results shown in Table I, it is evident that different brain connectivity features have a varying impact on the outcome for each category. Utilizing the participation coefficient yielded the most favourable results for the animal and vehicle categories. This finding suggests that the differentiation between object recognition and object identification for these categories is more discernible through the participation coefficient. On the other hand, the clustering coefficient didn't seem to provide significant outcomes for all the categories, implying that the difference between object recognition and object identification for these categories is not as distinguishable using the clustering coefficient. Despite this, the combination of the participation and clustering coefficients seems to impact the classification result positively. When combining both brain connectivity features, most of the classifiers demonstrated improvement for the animal, flower, and vehicle categories. Notably, the classification result for these three categories showed improvement across all classifiers except the XGBTress classifier for flower and vehicle categories when the combined features were utilized. This improvement implies that object recognition and object identification significantly differ in the participation and clustering coefficients for these three categories. The findings indicated that distinguishing between object recognition and object identification can be achieved by examining the participation and clustering coefficients as features.

Moreover, this participation coefficient and clustering coefficient at visual and temporal regions that can distinguish between object recognition and object identification has the potential to help us develop a better BCI system [13]. For example, this feature could be used within a BCI system to execute a classification algorithm depending on the user's objective. If the user's intention on an object is to want the BCI system to recognize the object, the BCI system could initiate an object recognition algorithm for object recognition ([26], [27], [28], [29], [17]) and provide feedback to the user. Rather, if the user wants to select an object within their environment, the BCI system could instead initiate an object identification algorithm for object identification ([21], [22], [23], [24], [25]) and select the desired target object. Such a BCI system could greatly help users with a disability to choose the object they want and communicate information about it with others.

D. Limitation

The findings of the functional connectivity analysis demonstrated notable differences between object recognition and object identification. However, several limitations within this analysis justify attention.

Firstly, the application of graph theory requires setting an arbitrary threshold to maintain the strongest connections consistently across subjects and to exclude spurious connections from connectivity matrices. This approach, while necessary, introduces the risk of incorporating false-positive and irrelevant connections. Given the variety of available thresholding methods, each with its potential biases, it is advisable to conduct analyses using different threshold values to verify the robustness of the results.

Secondly, EEG functional connectivity research continually grapples with the issue of the volume conduction effect [61]. Analyses at the source level have been effective in mitigating this issue, as they derive connectivity metrics from the time-series data of specific, localized brain regions. This method does reduce the volume conduction issue, but signal mixing may still occur in the cortical source space, potentially leading to false connections between brain regions by some connectivity methodologies. In this study, leakage correction methods like the Minimum Norm Estimate (MNE) have been used, which are designed to ensure that the reconstructed signals exhibit zero cross-correlation at lag zero [62]. While theoretically improving interpretation, recent research, such as that by Palva et al. [63], indicates that estimated connectivity might deviate significantly from actual connectivity.

Lastly, the study's participant count of 25, though substantial, is not sufficiently large to unequivocally validate the findings, be it in functional connectivity or binary classification outcomes. Future research should involve a greater number of participants to lend more credibility to the results.

V. Conclusion

In this study, we investigated neural dynamics to determine the underlying brain mechanisms at work during object recognition and identification. The results indicate a significant difference in the participation coefficient and clustering coefficient of delta activity in the brain's visual and temporal regions when engaged in object recognition as opposed to object identification. This adds to existing evidence that the visual and temporal regions of the brain play an essential role in recognizing and identifying objects. However, digging deeper into this phenomenon, we compared delta activity during both tasks at the category level and found

that different categories of objects spark different responses in the brain and that these categories differ between object recognition and identification. These results demonstrate that brain dynamics exhibit considerable variation between tasks of object recognition and identification, contingent on the nature of the objects involved. This observation is further corroborated by the outcomes of the binary classification analysis, which indicate that the neural features are less effective in the context of the food category. Such a difference between object recognition and identification could be an important feature of a BCI object recognition system, helping to pinpoint a user's objective when selecting a target object.

REFERENCES

[1] R. H. Masland and P. R. Martin, "The unsolved mystery of vision," *Current Biology*, vol. 17, no. 15, pp. R577–R582, 2007.

[2] E. D. Burgund and C. J. Marsolek, "invariant and viewpoint-dependent object recognition in dissociable neural subsystems," *Psychonomic Bulletin & Review*, vol. 7, no. 3, pp. 480–489, 2000.

[3] M. A. Peterson and G. Rhodes, *Perception of faces, objects, and scenes: Analytic and holistic processes*. Oxford University Press, 2003.

[4] M. J. Tarr and H. H. Bülthoff, "Is human object recognition better described by geon structural descriptions or by multiple views? comment on biederman and gerhardstein (1993)." 1995.

[5] M. A. Goodale and A. D. Milner, "Separate visual pathways for perception and action," *Trends in neurosciences*, vol. 15, no. 1, pp. 20–25, 1992.

[6] R. M. Cichy, D. Pantazis, and A. Oliva, "Resolving human object recognition in space and time," *Nature neuroscience*, vol. 17, no. 3, pp. 455–462, 2014.

[7] ——, "Similarity-based fusion of MEG and fMRI reveals spatio-temporal dynamics in human cortex during visual object recognition," *Cerebral Cortex*, vol. 26, no. 8, pp. 3563–3579, 2016.

[8] J. M. Shine, "Neuromodulatory influences on integration and segregation in the brain," *Trends in cognitive sciences*, vol. 23, no. 7, pp. 572–583, 2019.

[9] T.-T. N. Do, T.-P. Jung, and C.-T. Lin, "Retrosplenial Segregation Reflects the Navigation Load During Ambulatory Movement," *IEEE Transactions on Neural Systems and Rehabilitation Engineering*, vol. 29, pp. 488–496, 2021.

[10] R. Farivar, "Dorsal–ventral integration in object recognition," *Brain research reviews*, vol. 61, no. 2, pp. 144–153, 2009.

[11] M. M. van Ommen, A. Invernizzi, R. J. Renken, R. Bruggeman, F. Cornelissen, and T. van Laar, "Impaired functional connectivity in patients with psychosis and visual hallucinations," *medRxiv*, 2022.

[12] Y. Liu, C. Yu, M. Liang, J. Li, L. Tian, Y. Zhou, W. Qin, K. Li, and T. Jiang, "Whole brain functional connectivity in the early blind," *Brain*, vol. 130, no. 8, pp. 2085–2096, 2007.

[13] C.-T. Lin and T.-T. N. Do, "Direct-sense brain–computer interfaces and wearable computers," *IEEE Transactions on Systems, Man, and Cybernetics: Systems*, vol. 51, no. 1, pp. 298–312, 2020.

[14] J. Rizkallah, P. Benquet, A. Kabbara, O. Dufor, F. Wendling, and M. Hassan, "Dynamic reshaping of functional brain networks during visual object recognition," *Journal of neural engineering*, vol. 15, no. 5, p. 056022, 2018.

[15] Y. Han, K. Wang, J. Jia, and W. Wu, "Changes of EEG spectra and functional connectivity during an object-location memory task in Alzheimer's disease," *Frontiers in behavioral neuroscience*, vol. 11, p. 107, 2017.

[16] V. Rispoli, S. Ragusa, R. Nistico, R. Marra, E. Russo, A. Leo, V. Felicita, and D. Rotiroti, "Huperzine a restores cortico-hippocampal functional connectivity after bilateral ampa lesion of the nucleus basalis of meynert," *Journal of Alzheimer's Disease*, vol. 35, no. 4, pp. 833–846, 2013.

[17] T. F. Tafreshi, M. R. Daliri, and M. Ghodousi, "Functional and effective connectivity based features of EEG signals for object recognition," *Cognitive neurodynamics*, vol. 13, no. 6, pp. 555–566, 2019.

[18] M. Dyck and M. B. Brodeur, "Erp evidence for the influence of scene context on the recognition of ambiguous and unambiguous objects," *Neuropsychologia*, vol. 72, pp. 43–51, 2015.

[19] N. K. Logothetis and D. L. Sheinberg, "Visual object recognition," *Annual review of neuroscience*, vol. 19, no. 1, pp. 577–621, 1996.

[20] P. Rämä and T. Baccino, "Eye fixation–related potentials (efrps) during object identification," *Visual Neuroscience*, vol. 27, no. 5-6, pp. 187–192, 2010.

[21] B. Choi and S. Jo, "A low-cost EEG system-based hybrid brain-computer interface for humanoid robot navigation and recognition," *PloS one*, vol. 8, no. 9, p. e74583, 2013.

[22] F. Arrichiello, P. Di Lillo, D. Di Vito, G. Antonelli, and S. Chiaverini, "Assistive robot operated via p300-based brain computer interface," in *2017 IEEE International Conference on Robotics and Automation (ICRA)*. IEEE, 2017, pp. 6032–6037.

[23] K. Kaspar, U. Hassler, U. Martens, N. Trujillo-Barreto, and T. Gruber, "Steady-state visually evoked potential correlates of object recognition," *Brain research*, vol. 1343, pp. 112–121, 2010.

[24] X. Chen, B. Zhao, Y. Wang, and X. Gao, "Combination of high-frequency SSVEP-based BCI and computer vision for controlling a robotic arm," *Journal of neural engineering*, vol. 16, no. 2, p. 026012, 2019.

[25] S.-K. Chen, C.-S. Chen, Y.-K. Wang, and C.-T. Lin, "An SSVEP Stimuli Design using Real-time Camera View with Object Recognition," in *2020 IEEE Symposium Series on Computational Intelligence (SSCI)*. IEEE, 2020, pp. 562–567.

[26] A. M. Chan, E. Halgren, K. Marinkovic, and S. S. Cash, "Decoding word and category-specific spatiotemporal representations from MEG and EEG," *Neuroimage*, vol. 54, no. 4, pp. 3028–3039, 2011.

[27] C. Wang, S. Xiong, X. Hu, L. Yao, and J. Zhang, "Combining features from ERP components in single-trial EEG for discriminating four-category visual objects," *Journal of neural engineering*, vol. 9, no. 5, p. 056013, 2012.

[28] Y. Qin, Y. Zhan, C. Wang, J. Zhang, L. Yao, X. Guo, X. Wu, and B. Hu, "Classifying four-category visual objects using multiple ERP components in single-trial ERP," *Cognitive neurodynamics*, vol. 10, no. 4, pp. 275–285, 2016.

[29] M. Behroozi, M. R. Daliri, and B. Shekarchi, "EEG phase patterns reflect the representation of semantic categories of objects," *Medical & biological engineering & computing*, vol. 54, no. 1, pp. 205–221, 2016.

[30] G. Griffin, A. Holub, and P. Perona, "Caltech-256 object category dataset," 2007.

[31] A. Delorme and S. Makeig, "EEGLAB: an open source toolbox for analysis of single-trial EEG dynamics including independent component analysis," *Journal of neuroscience methods*, vol. 134, no. 1, pp. 9–21, 2004.

[32] L. Pion-Tonachini, K. Kreutz-Delgado, and S. Makeig, "Iclabel: An automated electroencephalographic independent component classifier, dataset, and website," *NeuroImage*, vol. 198, pp. 181–197, 2019.

[33] F. Tadel, S. Baillet, J. C. Mosher, D. Pantazis, and R. M. Leahy, "Brainstorm: a user-friendly application for MEG/EEG analysis," *Computational intelligence and neuroscience*, vol. 2011, 2011.

[34] V. S. Fonov, A. C. Evans, R. C. McKinstry, C. R. Almli, and D. Collins, "Unbiased nonlinear average age-appropriate brain templates from birth to adulthood," *NeuroImage*, no. 47, p. S102, 2009.

[35] A. Gramfort, T. Papadopoulo, E. Olivi, and M. Clerc, "OpenMEEG: opensource software for quasistatic bioelectromagnetics," *Biomedical engineering online*, vol. 9, no. 1, pp. 1–20, 2010.

[36] R. S. Desikan, F. Ségonne, B. Fischl, B. T. Quinn, B. C. Dickerson, D. Blacker, R. L. Buckner, A. M. Dale, R. P. Maguire, B. T. Hyman *et al.*, "An automated labeling system for subdividing the human cerebral cortex on mri scans into gyral based regions of interest," *Neuroimage*, vol. 31, no. 3, pp. 968–980, 2006.

[37] B. Fischl, "Freesurfer," *Neuroimage*, vol. 62, no. 2, pp. 774–781, 2012.

[38] R. D. Pascual-Marqui *et al.*, "Standardized low-resolution brain electromagnetic tomography (sloreta): technical details," *Methods Find Exp Clin Pharmacol*, vol. 24, no. Suppl D, pp. 5–12, 2002.

[39] J. F. Hipp, D. J. Hawellek, M. Corbetta, M. Siegel, and A. K. Engel, "Large-scale cortical correlation structure of spontaneous oscillatory activity," *Nature neuroscience*, vol. 15, no. 6, pp. 884–890, 2012.

[40] J. Rizkallah, J. Annen, J. Modolo, O. Gosseries, P. Benquet, S. Mortaheb, H. Amoud, H. Cassol, A. Mheich, A. Thibaut *et al.*, "Decreased integration of EEG source-space networks in disorders of consciousness," *NeuroImage: Clinical*, vol. 23, p. 101841, 2019.

[41] R. Zhang, L. Zhang, Y. Guo, L. Shi, J. Gao, X. Wang, and Y. Hu, "Effects of high-definition transcranial direct-current stimulation on resting-state functional connectivity in patients with disorders of consciousness," *Frontiers in human neuroscience*, vol. 14, p. 560586, 2020.

[42] H. Huang, Z. Niu, G. Liu, M. Jiang, Q. Jia, X. Li, and Y. Su, "Early consciousness disorder in acute large hemispheric infarction: an analysis based on quantitative eeg and brain network characteristics," *Neurocritical Care*, vol. 33, pp. 376–388, 2020.

[43] W. Zhuang, J. Wang, C. Chu, X. Wei, G. Yi, Y. Dong, and L. Cai, "Disrupted control architecture of brain network in disorder of consciousness," *IEEE Transactions on Neural Systems and Rehabilitation Engineering*, vol. 30, pp. 400–409, 2022.

[44] M. Rubinov and O. Sporns, "Complex network measures of brain connectivity: uses and interpretations," *Neuroimage*, vol. 52, no. 3, pp. 1059–1069, 2010.

[45] R. Guimera and L. A. Nunes Amaral, "Functional cartography of complex metabolic networks," *Nature*, vol. 433, no. 7028, pp. 895–900, 2005.

[46] D. J. Watts and S. H. Strogatz, "Collective dynamics of 'small-world'networks," *Nature*, vol. 393, no. 6684, pp. 440–442, 1998.

[47] F. Pedregosa, G. Varoquaux, A. Gramfort, V. Michel, B. Thirion, O. Grisel, M. Blondel, P. Prettenhofer, R. Weiss, V. Dubourg, J. Vanderplas, A. Passos, D. Cournapeau, M. Brucher, M. Perrot, and E. Duchesnay, "Scikit-learn: Machine learning in Python," *Journal of Machine Learning Research*, vol. 12, pp. 2825–2830, 2011.

[48] J. Snoek, H. Larochelle, and R. P. Adams, "Practical bayesian optimization of machine learning algorithms," *Advances in neural information processing systems*, vol. 25, 2012.

[49] M. Xia, J. Wang, and Y. He, "Brainnet viewer: a network visualization tool for human brain connectomics," *PloS one*, vol. 8, no. 7, p. e68910, 2013.

[50] H. Karimi-Rouzbahani, M. Shahmohammadi, E. Vahab, S. Setayeshi, and T. Carlson, "Temporal variabilities provide additional category-related information in object category decoding: a systematic comparison of informative EEG features," *Neural Computation*, vol. 33, no. 11, pp. 3027–3072, 2021.

[51] L. Hern andez-Andrade, A. C. Hermosillo-Abundis, B. L. Betancourt-Navarrete, D. Ruge, C. Trenado, R. Lemuz-L opez, H. J. Pelayo-Gonz alez, V. A. L opez-Cort es, M. d. R. Bonilla-S anchez, M. A. Garc ıa-Flores *et al.*, "EEG Global Coherence in Scholar ADHD Children during Visual Object Processing," *International Journal of Environmental Research and Public Health*, vol. 19, no. 10, p. 5953, 2022.

[52] A. J. Watrous, L. Deuker, J. Fell, and N. Axmacher, "Phase-amplitude coupling supports phase coding in human ecog," *Elife*, vol. 4, p. e07886, 2015.

[53] B. Cao, H. Niu, J. Hao, and G. Wang, "Building EEG-based CAD object selection intention discrimination model using convolutional neural network (CNN)," *Advanced Engineering Informatics*, vol. 52, p. 101548, 2022.

[54] K. Grill-Spector, "The neural basis of object perception," *Current opinion in neurobiology*, vol. 13, no. 2, pp. 159–166, 2003.

[55] A. Martin, C. L. Wiggs, L. G. Ungerleider, and J. V. Haxby, "Neural correlates of category-specific knowledge," *Nature*, vol. 379, no. 6566, pp. 649–652, 1996.

[56] M. S. Beauchamp, K. E. Lee, B. D. Argall, and A. Martin, "Integration of auditory and visual information about objects in superior temporal sulcus," *Neuron*, vol. 41, no. 5, pp. 809–823, 2004.

[57] A. Ishai, L. G. Ungerleider, A. Martin, J. L. Schouten, and J. V. Haxby, "Distributed representation of objects in the human ventral visual pathway," *Proceedings of the National Academy of Sciences*, vol. 96, no. 16, pp. 9379–9384, 1999.

[58] M. J. Farah and C. Rabinowitz, "Genetic and environmental influences on the organisation of semantic memory in the brain: Is "living things" an innate category?" *Cognitive Neuropsychology*, vol. 20, no. 3-6, pp. 401–408, 2003.

[59] B. Z. Mahon, S. Anzellotti, J. Schwarzbach, M. Zampini, and A. Caramazza, "Category-specific organization in the human brain does not require visual experience," *Neuron*, vol. 63, no. 3, pp. 397–405, 2009.

[60] M. L. Kringelbach, "The pleasure of food: underlying brain mechanisms of eating and other pleasures," *Flavour*, vol. 4, no. 1, pp. 1–12, 2015.

[61] C. Brunner, M. Billinger, M. Seeber, T. R. Mullen, and S. Makeig, "Volume conduction influences scalp-based connectivity estimates," *Frontiers in computational neuroscience*, vol. 10, p. 121, 2016.

[62] G. L. Colclough, M. J. Brookes, S. M. Smith, and M. W. Woolrich, "A symmetric multivariate leakage correction for meg connectomes," *Neuroimage*, vol. 117, pp. 439–448, 2015.

[63] J. M. Palva, S. H. Wang, S. Palva, A. Zhigalov, S. Monto, M. J. Brookes, J.-M. Schoffelen, and K. Jerbi, "Ghost interactions in meg/eeg source space: A note of caution on inter-areal coupling measures," *Neuroimage*, vol. 173, pp. 632–643, 2018.